RSC Advances

PAPER

View Article Online
View Journal | View Issue

Cite this: *RSC Adv.*, 2017, **7**, 18217

Selective turn-on near-infrared fluorescence probe for hypoxic tumor cell imaging†

Chen Jin,[a] Qiumeng Zhang[a] and Wei Lu *[ab]

Received 5th February 2017
Accepted 20th March 2017

DOI: 10.1039/c7ra01466j

rsc.li/rsc-advances

Hypoxia is a typical feature of solid tumors. To detect hypoxic tumor cells, we designed new selective turn-on probes by conjugating (1-methyl-2-nitro-1*H*-imidazol-5-yl)methanol to the near-infrared fluorescence probe **DCPO** through an ether linkage and bis-carbamate linkage specifically. The proposed activation mechanism was demonstrated through the nitroreductase and cytochrome P450 assays *in vitro*. However, two probes revealed different hypoxia selectivities when evaluated on H460, HeLa and A549 cell lines. The hypoxia selectivity of **IOD** was higher than that of **IND**. The probe **IOD** (containing the ether linkage) was considered to be a promising hypoxia-selective fluorescent probe.

Introduction

Hypoxia is a typical feature influencing many aspects of the biology of solid tumors. Most solid tumors have chronic hypoxic conditions within highly disorganized vascular networks since the intercapillary distances are often greater than the diffusion range of oxygen.[1] As the distance from the vessel changes, the oxygen tension, nutrients, cellular metabolites, cell proliferation, and extracellular pH gradients vary as well. Hypoxia affects many aspects of tumor biology including selection of genotypes favoring survival under a hypoxic microenvironment, pro-survival changes in gene expression that suppress apoptosis and support autophagy, and the anabolic switch in central metabolism.[2–6] These genetic alterations allow tumor cells to survive and even grow in such a harsh environment. Hypoxia is also an important contributor to tumor angiogenesis, vasculogenesis, invasiveness, metastasis, chemoresistance, and radioresistance.[7–9] Furthermore, owing to its unique features (which are rarely seen in normal tissue) hypoxia has been considered a primary target in cancer therapy.[10] Therefore, developing efficient methods for hypoxia detection is of great importance.

In solid tumors, the over-expressed reductive enzyme level corresponds with the hypoxic status. 2-Nitroimidazole has been demonstrated to be converted to 2-aminoimidazole *via* a series of bioreductions in hypoxic microenvironments.[11–16] 2-Nitroimidazole-based derivatives including pimonidazole,[17] EF5,[18] ^{18}F-FMISO, and ^{18}F-FAZA[19] (Fig. 1) have been used to selectively label the hypoxic area of tumors *via* PET (positron emission tomography). However, the disadvantage that a radioactive tracer must be injected into patients is the main problem with PET.

Near-infrared (NIR) fluorescent dyes have been widely used for monitoring biological processes in cells and organisms.[20–28] In general, NIR fluorophores emit fluorescence in the range of 650–900 nm. Compared with PET, NIR probes possess the advantages of minimal photo-damage to biological samples, deep tissue penetration, and low background auto-fluorescence. (*E*)-2-(2-(4-Hydroxystyryl)-4*H*-chromen-4-ylidene)malononitrile (**DCPO**) and its derivatives are photostable and widely used in the detection of cathepsin B, hydrogen peroxide, and GLUT-1.[29–34]

Several works have reported the targeting of hypoxic tumors with turn-on fluorescent probes containing a bioreductive nitro group or azo group.[35–42] However, (1-methyl-2-nitro-1*H*-imidazol-5-yl)methanol, which was applied in the clinical hypoxia-activated prodrug evofosfamide (TH-302)[43] and considered an effective bioreductive molecule, has been sparingly used in the development of hypoxia imaging. Recently, Grimm reported a dual-input fluorogenic probe using (1-methyl-2-nitro-1*H*-imidazol-5-yl)methanol.[44] Though the probe was demonstrated to be

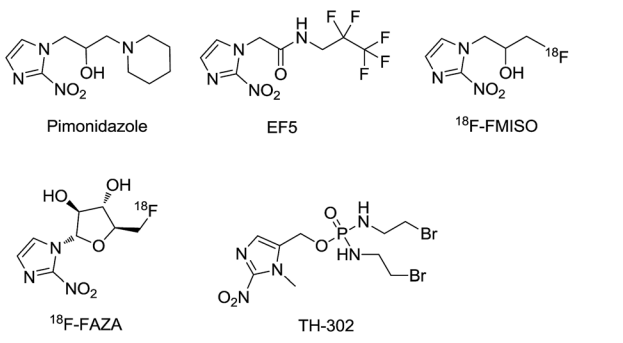

Fig. 1 Chemical structures of pimonidazole, EF5, ^{18}F-FMISO, ^{18}F-FAZA and evofosfamide (TH-302).

[a]*School of Chemistry and Molecular Engineering, East China Normal University, 3663 North Zhongshan Road, Shanghai 200062, P. R. China. E-mail: wlu@chem.ecnu.edu.cn; Tel: +86-21-62238771*

[b]*State Key Laboratory of Fine Chemicals, Dalian University of Technology, Dalian 116024, P. R. China*

† Electronic supplementary information (ESI) available. See DOI: 10.1039/c7ra01466j

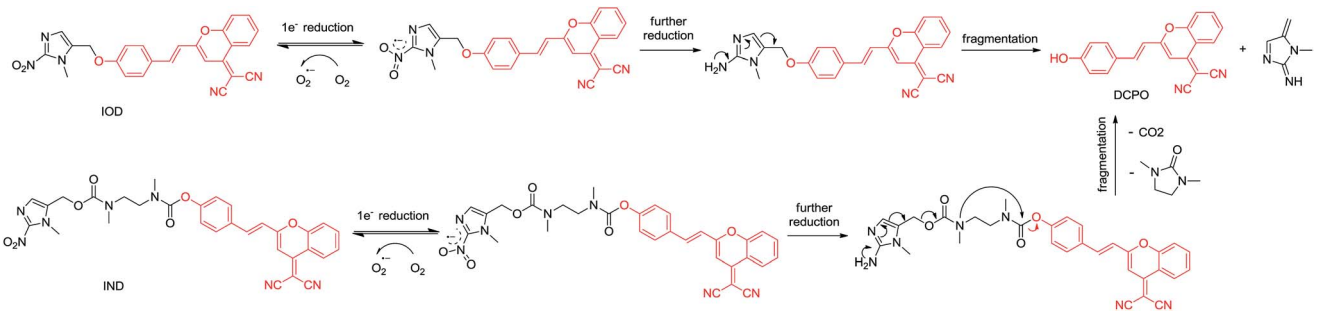

Fig. 2 Proposed mechanism of probes activated *via* enzymatic metabolism under hypoxic condition.

effective *via* the bioreduction of nitroreductase, it did not investigate the selectivity between hypoxic and normoxic cell imaging.

In this paper, we proposed new hypoxic fluorescent probes based on (1-methyl-2-nitro-1*H*-imidazol-5-yl)methanol. The near-infrared fluorescence OFF–ON switch could be triggered by nitroimidazole *via* the transformation of a masked phenol unit to a phenolic hydroxyl group. In normal tissues, no fluorescence was observed *via* the Förster resonance energy transfer (FRET) mechanism caused by the electron acceptor nitro group. Conversely, in hypoxic solid tumors, the hypoxia-specific nitro-to-amino reduction activated the nitroimidazole trigger and generated red-fluorescence (Fig. 2). The ether linkage and bis-carbamate linkage were specifically used to connect (1-methyl-2-nitro-1*H*-imidazol-5-yl)methanol and **DCPO**. The most important of this study was that, two fluorescent probes revealed different properties upon biological evaluation. Probe **IOD** containing ether linkage was evaluated to be better than probe **IND** containing bis-carbamate linkage.

Experimental

Material and methods

^{1}H and ^{13}C nuclear magnetic resonance (NMR) spectra were recorded on a Bruker DRX-400 MHz spectrometer (400 and 101 MHz, respectively) using $CDCl_3$, or DMSO-d_6 as solvents with TMS as an internal standard. Chemical shifts were reported as d (ppm) and spin–spin coupling constants as *J* (Hz) values. The mass spectra (MS) were recorded on a Finnigan MAT-95 mass spectrometer. Melting points were taken on a SGW X-4 melting point apparatus, uncorrected and reported in degrees centigrade. Column chromatography was performed with silica gel (200–300 mesh). UV-vis absorption spectra were recorded on a Varian Cary 100 spectrophotometer. Fluorescence spectra were measured with a Hitachi F-4500 Fluorescence spectrophotometer. Cells were taken photos on an inverted fluorescence microscope (Olympus DP80). The average fluorescence intensity was given by the flow cytometry assay on a Guava easyCyte HT system.

Nitroreductase from *Escherichia coli* and NADPH were purchased from Sigma-Aldrich. Mouse liver microsomes (20 mg mL^{-1}) were purchased from Corning. Human lung cancer cell line H460, human cervical cancer cell line HeLa and human lung adenocarcinoma cell line A549 were purchased from the Shanghai Institute of Biochemistry and Cell Biology (Shanghai, China). The cell culture fluid and FBS were purchased from Thermo Fisher Scientific. All of the starting materials are commercially available and were used without further purification.

Ethical statement

We state that all experiments with live subjects were performed in compliance with the Laboratory Animal Management Regulations of the People's Republic of China and the Three Rs (Replacement, Reduction, and Refinement) strategy of William Russell and Rex Burch, and the Animal Ethical and Welfare Committee of East China Normal University has approved the experiments.

Synthetic procedures

Compound 1. Compound **1** was synthesized according to the procedure of Duan *et al.*[43]

Compound 2. To a stirred solution of compound **1** (47 mg, 0.3 mmol) and DMAP (73 mg, 0.6 mmol) in DCM (3 mL) was added TsCl (69 mg, 0.36 mmol). The reaction was stirred for 4 h at room temperature. The mixture was concentrated in vacuum and purified by column chromatography on silica gel (heptane : EtOAc = 10 : 1) to afford compound **2** (50 mg, 95%) as yellow solid. Mp 96–98 °C. ^{1}H NMR (400 MHz, $CDCl_3$) δ 7.19 (s, 1H), 4.62 (s, 2H), 4.07 (s, 3H). MS (ESI): *m*/*z* calcd for $C_5H_7ClN_3O_2$ $[M + H]^+$: 175.01, found: 175.87.

Compound 3. To a stirred solution of 4-hydroxybenzaldehyde (42 mg, 0.34 mmol) in DMF (3 mL) was added K_2CO_3 (40 mg, 0.29 mmol) and compound **2** (50 mg, 0.29 mmol). The mixture was stirred overnight at 60 °C. The reaction was quenched with H_2O and extracted with EtOAc. The combined organic layers were dried over Na_2SO_4. Concentration was purified by column chromatography on silica gel (heptane : EtOAc = 1 : 1) to afford compound **3** (65 mg, 86%) as yellow solid. Mp 181–183 °C. ^{1}H NMR (400 MHz, $CDCl_3$) δ 9.92 (s, 1H), 7.88 (d, J = 8.4 Hz, 2H), 7.25 (s, 1H), 7.08 (d, J = 8.4 Hz, 2H), 5.14 (s, 2H), 4.07 (s, 3H). ^{13}C NMR (101 MHz, $CDCl_3$) δ 190.7, 162.6, 162.2, 132.2, 131.8, 131.1, 129.3, 115.0, 59.7, 36.6, 34.6, 31.5. MS (ESI): *m*/*z* calcd for $C_{12}H_{12}N_3O_4$ $[M + H]^+$: 261.08, found: 261.86.

Compound 5 (IOD). Compound **3** (30 mg, 11 mmol) and compound **4** (27 mg, 0.13 mmol) was dissolved in acetonitrile (4 mL), then followed by adding HOAc (0.2 mL), piperidine

(0.2 mL) in sequence. The reaction was stirred overnight at 80 °C, then quenched with water and extracted with DCM. The combined organic layers were dried over Na_2SO_4. Concentration was purified by column chromatography on silica gel (DCM : MeOH = 50 : 1) to afford compound **5** (22 mg, 44%) as red solid. Mp > 300 °C. ^{1}H NMR (400 MHz, DMSO) δ 8.73 (d, J = 8.2 Hz, 1H), 7.97–7.88 (m, 1H), 7.84–7.69 (m, 4H), 7.65–7.58 (m, 1H), 7.45–7.35 (m, 2H), 7.19 (d, J = 8.6 Hz, 2H), 7.00 (s, 1H), 5.34 (s, 2H), 3.96 (s, 3H). ^{13}C NMR (101 MHz, DMSO) δ 159.4, 158.5, 152.9, 152.0, 146.3, 138.4, 135.4, 133.2, 130.0, 128.6, 128.5, 126.1, 124.6, 119.0, 117.6, 117.3, 117.1, 115.9, 115.6, 106.2, 59.7, 59.3, 34.4. HRMS (ESI): m/z calcd for $C_{25}H_{17}N_5O_4Na$ $[M + Na]^+$: 474.1178, found: 474.1177.

Compound 6. To a stirred solution of compound **1** (30 mg, 0.19 mmol) and DIPEA (49 mg, 0.38 mmol) in DCM (5 mL) was added bis(4-nitrophenyl)carbonate (64 mg, 0.21 mmol). The reaction was stirred for 4 h at room temperature, then was added *N*,*N*′-dimethyl-*N*-tritylethane-1,2-diamine (94 mg, 0.29 mmol). The mixture was stirred for another 1 h. Then the solution was washed with Na_2CO_3 and extracted with DCM. The combined organic layers were dried over Na_2SO_4. Concentration was purified by column chromatography on silica gel (heptane : EtOAc = 2 : 1) to afford compound **6** (88 mg, 91%) as yellow solid. Mp 100–102 °C. ^{1}H NMR (400 MHz, $CDCl_3$) δ 7.50–7.37 (m, 6H), 7.26–7.19 (m, 6H), 7.18–7.11 (m, 3H), 7.08 (s, 1H), 5.19–5.01 (m, 2H), 4.05–3.62 (m, 3H), 3.56–3.37 (m, 2H), 3.13–2.89 (m, 3H), 2.38–2.18 (m, 2H), 2.18–2.05 (m, 3H). MS (ESI): m/z calcd for $C_{29}H_{32}N_5O_4$ $[M + H]^+$: 514.24, found: 514.37.

Compound 7. To a stirred solution of compound **6** (51 mg, 0.1 mmol) in DCM (2 mL) was added trifluoroacetic acid (0.2 mL). The reaction was stirred for 1 h at room temperature, and concentrated in vacuum to produce the crude product of compound **7**, which was used in the next step without purification.

Compound 9. Under N_2 atmosphere, to a stirred solution of compound **8** (31 mg, 0.1 mmol) and triphosgene (15 mg, 0.05 mmol) in dry DCM (10 mL) was added DIPEA (39 mg, 0.3 mmol) dropwise at 0 °C. Then the reaction was stirred at room temperature overnight and put into next step without purification.

Compound 10 (IND). To a stirred solution of crude compound **7** in DCM (2 mL) was added appropriate DIPEA to keep pH among 7–8. Then the solution of compound **9** was added into the reaction and stirred at room temperature for 2 h. The mixture was concentrated in vacuum and purified by column chromatography on silica gel (DCM : MeOH = 30 : 1) to afford compound **10** (24 mg, 39%) as red solid. Mp > 300 °C. ^{1}H NMR (400 MHz, $CDCl_3$) δ ^{1}H NMR (400 MHz, $CDCl_3$) δ 8.92 (d, J = 8.3 Hz, 1H), 7.79–7.71 (m, 1H), 7.66–7.51 (m, 4H), 7.50–7.41 (m, 1H), 7.24–6.99 (m, 3H), 6.88 (s, 1H), 6.82–6.73 (m, 1H), 5.23–5.08 (m, 2H), 4.10–3.90 (m, 3H), 3.70–3.42 (m, 4H), 3.20–2.87 (m, 6H). ^{13}C NMR (101 MHz, $CDCl_3$) δ 157.4, 155.6, 154.6, 154.1, 152.9, 152.4, 146.2, 137.9, 134.8, 123.0, 129.7, 129.5, 129.1, 129.04, 126.1, 125.9, 122.3, 118.8, 117.9, 116.9, 115.7, 107.0, 62.9, 56.0, 47.5, 34.4, 29.8. HRMS (ESI): m/z calcd for $C_{31}H_{27}N_7O_7Na$ $[M + Na]^+$: 632.1870, found: 632.1899.

General HPLC method

HPLC analysis was performed at room temperature using a Diamonsil C_{18} (250 mm × 4.6 mm) and a mobile phase gradient from 5% CH_3CN/buffer (0.1% TFA/H_2O) to 70% CH_3CN/buffer (0.1% TFA/H_2O) for 5 min, 70% CH_3CN/buffer (0.1% TFA/H_2O) to 95% CH_3CN/buffer (0.1% TFA/H_2O) for 10 min, 95% CH_3CN/buffer (0.1% TFA/H_2O) for 5 min, a flow rate of 1.0 mL min^{-1}, and plotted at 440 nm. This method was used to determine the purity for the tested compounds, and also used in stability studies.

General method for nitroreductase assay and cytochrome P450 metabolism assay

The probe measurements were made in 10 mM PBS (pH 7.4, 1% DMSO). The incubation mixtures of test probes with nitroreductase contained the following at the indicated final concentrations: 10 μM test compound, nitroreductase (50 μg mL^{-1}) and 1 mM NADPH. The incubation mixtures of test probes with mouse liver microsomes contained the following at the indicated final concentrations: 25 μM test compound, 5 mM $MgCl_2$, mouse liver microsomes (50 μg mL^{-1}) and 1 mM NADPH. The mixtures were incubated at 37 °C. At different time, 100 μL reaction mixture was quenched by 100 μL cold methanol. The samples were centrifuged at 4 °C for 5 min at 12 000 rpm. The supernatant was transferred to a vial for analysis using HPLC.

Cell culture and imaging

H460, HeLa, A549 were cultured in RPMI 1640 medium, DMEM medium, F12 medium, supplemented with 10% fetal bovine serum and 1% penicillin streptomycin in a 5% CO_2 humidified environment at 37 °C. Cells were seeded in 96-well plates and incubated for 24 h. The next day, test probes in DMSO were diluted in medium with final concentration of 10 μM (1% DMSO). The cells in the hypoxia treatment group were incubated for 24 h in the anaerobic chamber flushed with a certified anaerobic gas mixture (94% N_2/5% CO_2/1% O_2; Thermo). The cells in the air treatment group were incubated for 24 h in standard cell-culture incubator. After appropriate time of treatment with test compounds, the cells were washed with 200 μL PBS three times and fixed with 4% paraformaldehyde. Finally, 100 μL of PBS was added and the cells were visualized on an inverted fluorescence microscope (Olympus DP80) with green exciting light. The fluorescence images were taken under a 20× objective. The average fluorescence intensity was detected at 661 nm and excited at 640 nm by the flow cytometry assay on a Guava easyCyte HT system.

Results and discussion

Chemistry

Compound **1** was reacted with TsCl in the presence of DMAP to prepare compound **2**. Then, 4-hydroxybenzaldehyde was reacted with compound **2** in K_2CO_3/DMF to afford compound **3**. Compounds **3** and **4** were refluxed in acetonitrile with HOAc and piperidine to produce compound **5** (**IOD**) with 36% overall

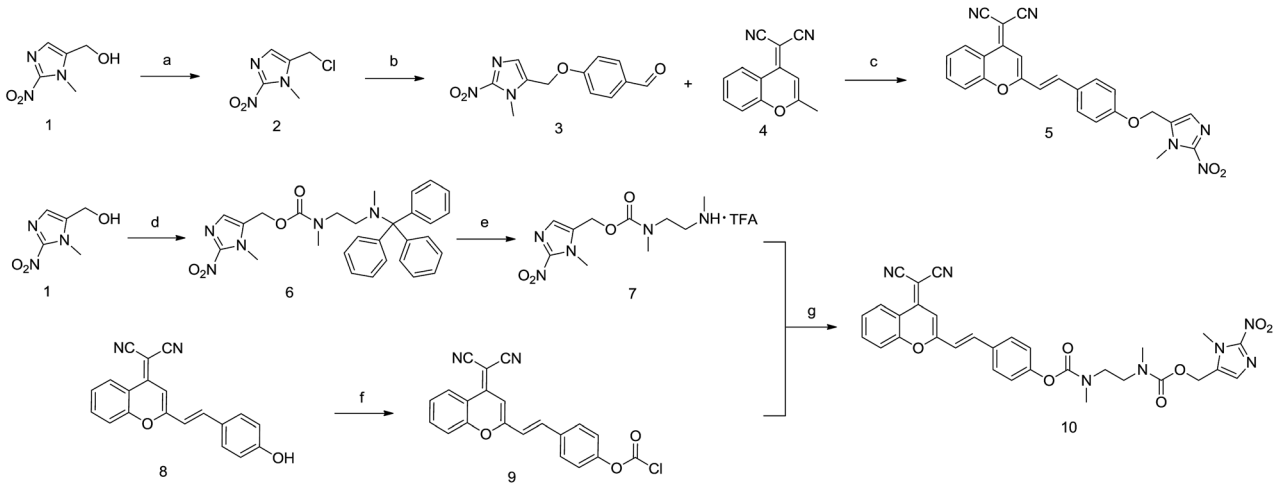

Scheme 1 Reagents and conditions: (a) TsCl, DMAP, DCM; (b) K_2CO_3, DMF; (c) HOAc, piperidine, acetonitrile; (d) bis(4-nitrophenyl)carbonate, *N*,*N*′-dimethyl-*N*-tritylethane-1,2-diamine, DIPEA, DCM; (e) 10% TFA/DCM; (f) triphosgene, DIPEA, DCM; (g) DIPEA, DCM.

yield. On the other hand, compound **1** was treated with bis(4-nitrophenyl)carbonate followed by the addition of *N*-trityl-*N*,*N*′-dimethylethylenediamine to produce compound **6**. The trityl protecting group was removed in 10% TFA/DCM to afford compound 7. **DCPO** was reacted with triphosgene/DIPEA, followed by the addition of the solution of compound 7 to synthesize compound **10** (**IND**) with 35% overall yield (Scheme 1).

Optical properties of probes

We tested the optical properties of the probe (**IOD**/**IND**) in PBS buffer (10 mM, pH 7.4, 50% DMSO). The main absorption peak of **DCPO** appeared at 560 nm while low absorption peaks of **IOD**/**IND** were observed at 560 nm (Fig. 3). As expected, the fluorescence of the probe was eliminated when the phenol moiety was masked with nitroimidazole.

In vitro nitroreductase assay

We proposed that both **IOD** and **IND** could be reduced to the original fluorescent probe **DCPO**. To testify whether the probes could be activated and fragmented, nitroreductase (NTR) from *Escherichia coli* was used. The probes dissolved in PBS (5 μM, PBS buffer with 1% DMSO) were incubated with nitroreductase (50 μg mL^{-1}) and NADPH (1 μmol mL^{-1}) at 37 °C. The reduction processes of **IOD** and **IND** were monitored through HPLC (Fig. 4). However, the two probes revealed different properties. The results indicated that **IND** was completely reduced and almost converted to **DCPO** at 15 min. On the other hand, 42% of **IOD** was still remaining at 15 min. We supposed that both probes underwent the bioreductive processes, as we proposed. Due to the reversible reaction in the first step under the normoxic condition, it was more reasonable to have 42% of **IOD** remaining.

In vitro cytochrome P450 metabolism assay

Though the probes could be reduced by bioreductase, it was necessary to testify whether the probes could be stable in the presence of other enzymes. As we know, many prodrugs and

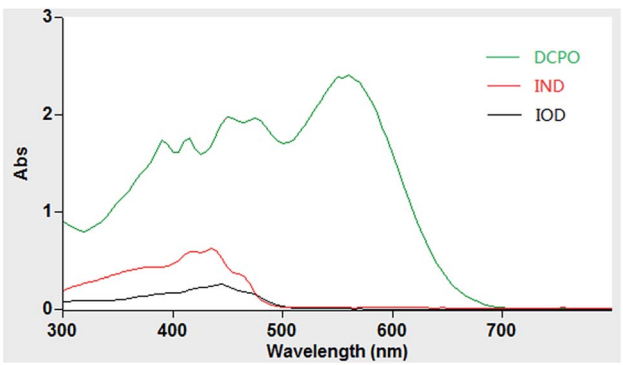

Fig. 3 Absorption spectra of **DCPO**, **IOD** and **IND**, 25 μM in PBS buffer (10 mM, pH 7.4, 50% DMSO).

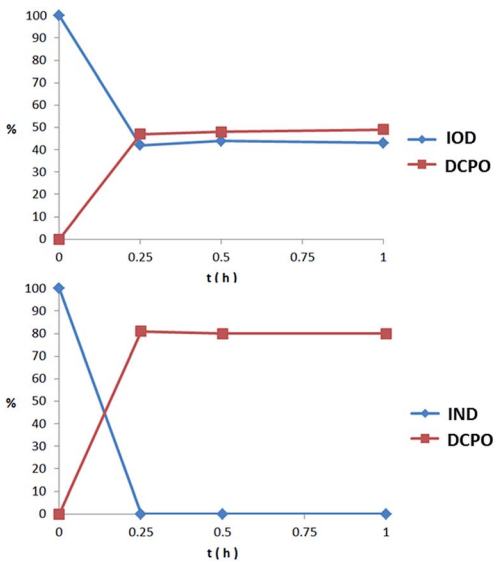

Fig. 4 Percent of probe remaining and **DCPO** releasing in 1 h incubation with nitroreductase (50 μg mL^{-1}) and NADPH (1 μmol mL^{-1}) at 37 °C.

Table 1 *In vitro* stability of probes

	NTR[a]		MLM[b]	
	Compound remaining	**DCPO** release	Compound remaining	**DCPO** release
IOD	42	47	48	43
IND	0	81	2	30

[a] Percent of probe remaining and **DCPO** releasing in 1 h of incubation with nitroreductase (50 μg mL^{-1}) and NADPH (1 μmol mL^{-1}) at 37 °C. [b] Percent of probe remaining and **DCPO** releasing in 24 h of incubation with mouse liver microsomes (50 μg mL^{-1}) and NADPH (1 μmol mL^{-1}) at 37 °C.

probes undergo oxidation and reduction metabolism by cytochrome P450. Cytochrome P450, which is the main component of animals' liver microsomal enzyme, was used to test the metabolism of the probes. Mouse liver microsomes (50 μg mL^{-1}) and NADPH (1 μmol mL^{-1}) were added to the **IOD**/**IND** solution (25 μM, PBS buffer with 1% DMSO) and incubated at 37 °C for 24 h. The results were detected using HPLC (Table 1). The quantity of **IOD** remaining and **DCPO** released in the mouse liver microsome assay was similar to that in the nitroreductase assay. However, **IND** showed a distinct difference in **DCPO** release. The HPLC results indicated that **IND** was converted to other **DCPO** derivatives and the quantity of **DCPO** released was much lower. The fluorescence emissions of the probes after incubation with mouse liver microsomes for 24 h are shown in Fig. 5, which also indicates that **IOD** had a stronger emission than **IND**. We hypothesized that **IOD** underwent bioreductive metabolism, as we proposed previously. However, **IND** underwent a more complicated metabolic process, maybe because the bis-carbamate linkage could be a substrate for other enzymes besides the reductase in cytochrome P450.

Fluorescence imaging in H460, HeLa, A549 cell lines

The probes were evaluated under normoxic and hypoxic (94% N_2/5% CO_2/1% O_2) conditions using H460, HeLa and A549 cell lines. The probes **IOD** and **IND** (10 μM, 1% DMSO) were co-cultivated with cells at 37 °C under hypoxic and normoxic conditions for different lengths of time.

As shown in Fig. 6, time-dependent fluorescence enhancement was observed under hypoxic conditions, while fluorescence changes under normoxic conditions were not as obvious as hypoxic conditions. In each cell line, probe **IOD** was observed

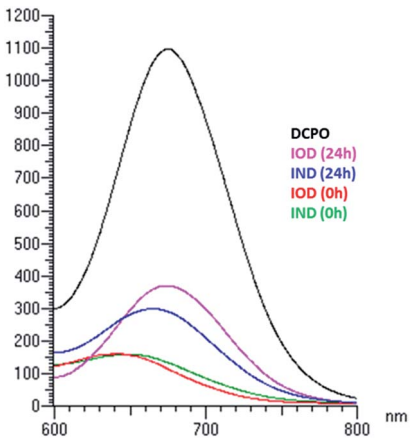

Fig. 5 Emission spectra of probes (25 μM) excited at 560 nm after 24 h incubation with mouse liver microsomes (50 μg mL^{-1}) and NADPH (1 μmol mL^{-1}) at 37 °C.

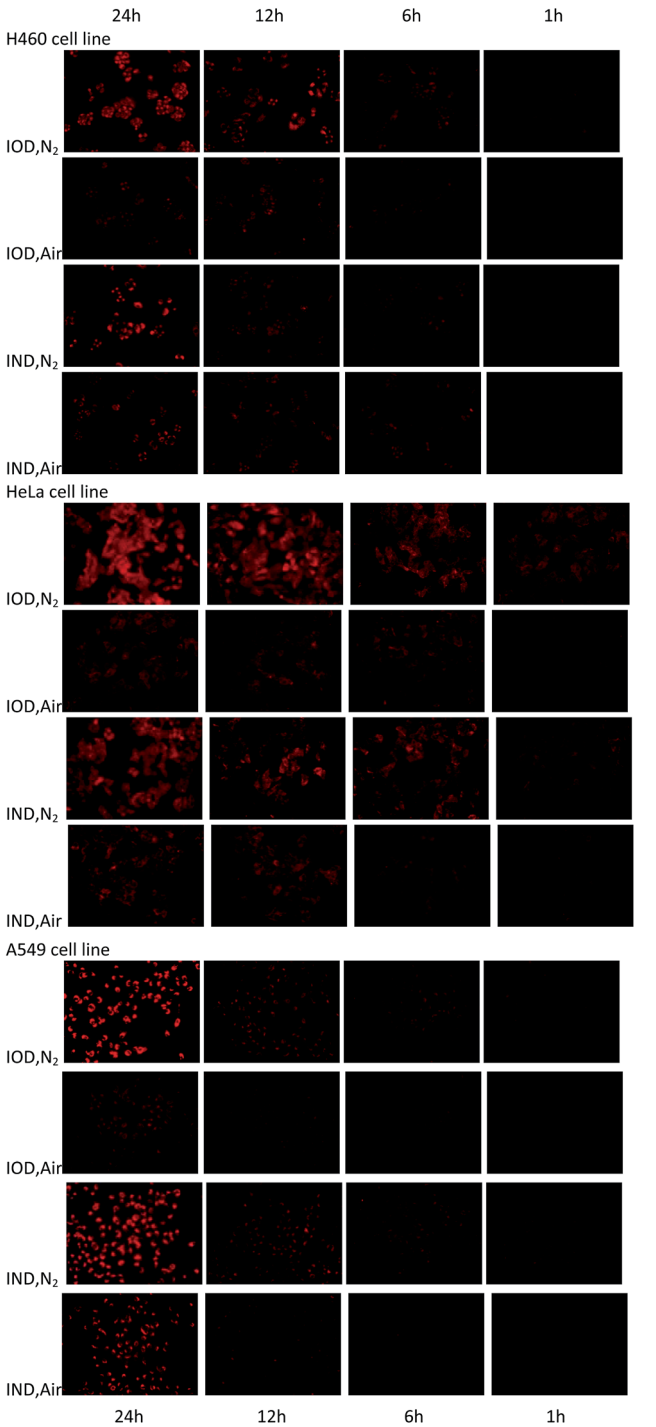

Fig. 6 Fluorescence field microphotographs of H460, HeLa and H460 cells incubated with 10 μM probe under normoxic and hypoxic condition (94% N_2/5% CO_2/1% O_2) for different time.

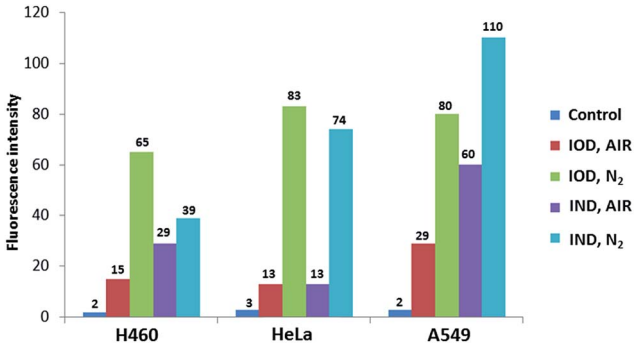

Fig. 7 The average fluorescence intensity of H460, HeLa, A549 cells detected at 661 nm and excited at 640 nm.

to have greater difference between hypoxic and normoxic cells. The average fluorescence intensity after 24 h incubation was given by the flow cytometry assay on a Guava easyCyte HT system (Fig. 7). The quantified results indicated that, probe **IOD** had a higher hypoxia selectivity ratio than **IND** in each cell line.

The cytotoxicity of probes was investigated on three cell lines. The results indicated that, the probes had no obvious inhibition towards three cell lines in both hypoxic and normoxic condition (Fig. S2†).

Conclusions

In this study, we synthesized two probes based on (1-methyl-2-nitro-1*H*-imidazol-5-yl)methanol and **DCPO**. Biological evaluation indicated that different linkages revealed distinctly different results. Probe **IOD** with an ether linkage was demonstrated to be able to release **DCPO** *via* metabolism by nitroreductase and cytochrome P450. However, probe **IND** with a biscarbamate linkage may be a substrate to enzymes beyond the reductase in cytochrome P450. The hypoxia selectivity ratio of **IOD** was evaluated to be higher than that of **IND** on H460, HeLa and A549 cell lines. In conclusion, the probe **IOD** was considered to be a promising hypoxia-selective fluorescent probe.

Acknowledgements

The authors are grateful for the financial support from the State Key Laboratory of Fine Chemicals, Dalian University of Technology (KF1517).

Notes and references

1 J. M. Brown, *Cancer Biol. Ther.*, 2002, **1**, 453–458.
2 W. R. Wilson and M. P. Hay, *Nat. Rev. Cancer*, 2011, **11**, 393–410.
3 R. A. Cairns, I. S. Harris and T. W. Mak, *Nat. Rev. Cancer*, 2011, **11**, 85–95.
4 T. G. Graeber, C. Osmanian, T. Jacks, D. E. Housman, C. J. Koch, S. W. Lowe and A. J. Giaccia, *Nature*, 1996, **379**, 88–91.
5 J. T. Erler, C. J. Cawthorne, K. J. Williams, M. Koritzinsky, B. G. Wouters, C. Wilson, C. Miller, C. Demonacos, I. J. Stratford and C. Dive, *Mol. Cell. Biol.*, 2004, **24**, 2875–2889.
6 K. M. Rouschop, B. T. Van, L. Dubois, H. Niessen, J. Bussink, K. Savelkouls, T. Keulers, H. Mujcic, W. Landuyt, J. W. Voncken, P. Lambin, A. J. Kogel, M. Koritzinsky and B. G. Wouters, *J. Clin. Invest.*, 2010, **120**, 127–141.
7 Y. Wang and M. Ohh, *J. Cell. Mol. Med.*, 2010, **14**, 496–503.
8 R. D. Guzy, B. Hoyos, E. Robin, H. Chen, L. P. Liu, K. D. Mansfield, M. C. Simon, U. Hammerling and P. T. Schumacker, *Cell Metab.*, 2005, **1**, 401–408.
9 J. M. Brown and W. R. Wilson, *Nat. Rev. Cancer*, 2004, **4**, 437–447.
10 G. O. Ahn and M. Brown, *Front. Biosci.*, 2007, **12**, 3483–3501.
11 R. M. Phillips, *Cancer Chemother. Pharmacol.*, 2016, **77**, 441–457.
12 T. Thambi, J. H. Park and D. S. Lee, *Chem. Commun.*, 2016, **52**, 8492–8500.
13 A. J. Lin, L. A. Cosby, C. W. Shansky and A. C. Sartorelli, *J. Med. Chem.*, 1973, **15**, 1247–1252.
14 S. R. McKeown, R. L. Cowen and K. J. Williams, *Clin. Oncol.*, 2007, **19**, 427–442.
15 R. P. Mason and J. L. Holtzman, *Biochem. Biophys. Res. Commun.*, 1975, **67**, 1267–1274.
16 E. Nieto, M. Delgado, M. Sobrado, M. L. Ceballos, R. Alajarín, L. G. García, J. Kelly, I. Lizasoain and M. A. Pozo, *Eur. J. Med. Chem.*, 2015, **101**, 604–615.
17 K. L. Bennewith, J. A. Raleigh and R. E. Durand, *Cancer Res.*, 2002, **62**, 6827–6830.
18 S. M. Evans, K. D. Judy, I. Dunphy, W. T. Jenkins, P. T. Nelson, R. Collins, E. P. Wileyto, K. Jenkins, S. M. Hahn, C. W. Stevens, A. R. Judkins, P. Phillips, B. Geoerger and C. J. Koch, *Cancer Res.*, 2004, **64**, 1886–1892.
19 J. G. Rajendran and D. A. Mankoff, *J. Nucl. Med.*, 2007, **48**, 855–856.
20 Z. Guo, S. Park, J. Yoon and I. Shin, *Chem. Soc. Rev.*, 2014, **43**, 16–29.
21 A. R. Lippert, G. C. Van de Bittner and C. J. Chang, *Acc. Chem. Res.*, 2011, **44**, 793–804.
22 Y. Yang, Q. Zhao, W. Feng and F. Li, *Chem. Rev.*, 2012, **113**, 192–270.
23 S. A. Hilderbrand and R. Weissleder, *Curr. Opin. Chem. Biol.*, 2010, **14**, 71–79.
24 G. Bazar, V. Eles, Z. Kovacs, R. Romvari and A. Szabo, *Talanta*, 2016, **155**, 202–211.
25 R. Risoluti, S. Materazzi, A. Gregori and L. Ripani, *Talanta*, 2016, **153**, 407–413.
26 L. He, B. Dong, Y. Liu and W. Lin, *Chem. Soc. Rev.*, 2016, **45**, 6449–6461.
27 X. Chen, Y. Zhou, X. Peng and J. Yoon, *Chem. Soc. Rev.*, 2010, **39**, 2120–2135.
28 J. Du, M. Hu, J. Fan and X. Peng, *Chem. Soc. Rev.*, 2012, **41**, 4511–4535.
29 X. Zhang, L. Zhang, Y. Liu, B. Bao, Y. Zang, J. Li and W. Lu, *Tetrahedron*, 2015, **71**, 4842–4845.

30 B. Bao, Y. Liu, L. Wang and W. Lu, *RSC Adv.*, 2016, **6**, 69540–69545.
31 S. Chen, Y. Fang, Q. Zhu, W. Zhang, X. Zhang and W. Lu, *RSC Adv.*, 2016, **6**, 81894–81901.
32 Z. Lu, J. Wu, W. Liu, G. Zhang and P. Wang, *RSC Adv.*, 2016, **6**, 32046–32051.
33 P. Wang, K. Wang, D. Chen, Y. Mao and Y. Gu, *RSC Adv.*, 2015, **5**, 85957–85963.
34 J. Cao, C. Zhao and W. Zhu, *Tetrahedron Lett.*, 2012, **53**, 2107–2110.
35 T. Guo, L. Cui, J. Shen, W. Zhu, Y. Xu and X. Qian, *Chem. Commun.*, 2013, **49**, 10820–10822.
36 J. Zhou, W. Shi, L. Li, Q. Gong, X. Wu, X. Li and H. Ma, *Chem.–Asian J.*, 2016, **11**, 2719–2724.
37 Q. Cai, T. Yu, W. Zhu, Y. Xu and X. Qian, *Chem. Commun.*, 2015, **51**, 14739–14741.
38 J. Rao and A. Khan, *J. Am. Chem. Soc.*, 2013, **135**, 14056–14059.
39 J. Rao, C. Hottinger and A. Khan, *J. Am. Chem. Soc.*, 2014, **136**, 5872–5875.
40 K. Okuda, Y. Okabe, T. Kadonosono, T. Ueno, B. G. M. Youssif, S. K. Kondoh and H. Nagasawa, *Bioconjugate Chem.*, 2012, **23**, 324–329.
41 Q. Lin, C. Bao, Y. Yang, Q. Liang, D. Zhang, S. Cheng and L. Zhu, *Adv. Mater.*, 2013, **25**, 1981–1986.
42 K. Xu, F. Wang, X. Pan, R. Liu, J. Ma, F. Kong and B. Tang, *Chem. Commun.*, 2013, **49**, 2554–2556.
43 J. X. Duan, H. Jiao, J. Kaizerman, T. Stanton, J. W. Evans, L. Lan, G. Lorente, M. Banica, D. Jung, J. Wang, H. Ma, X. Li, Z. Yang, R. M. Hoffman, W. S. Ammons, C. P. Hart and M. Matteucci, *J. Med. Chem.*, 2008, **51**, 2412–2420.
44 J. B. Grimm, T. D. Gruber, G. Ortiz, T. A. Brown and L. D. Lavis, *Bioconjugate Chem.*, 2016, **27**, 474–480.